Macromolecules

Article

pubs.acs.org/Macromolecules

Effects of Intrachain Interactions on the Knot Size of a Polymer

Liang Dai[†] and Patrick S. Doyle*[,†,‡]

[†]BioSystems and Micromechanics IRG, Singapore-MIT Alliance for Research and Technology Centre, Singapore 117543

[‡]Department of Chemical Engineering, Massachusetts Institute of Technology (MIT), Cambridge, Massachusetts 02139, United States

Supporting Information

ABSTRACT: Knots occur frequently in our daily life and also in long polymers. Studies of spontaneously occurring knots in a linear polymer have focused on their size and probabilities. In this work, we report counterintuitive phenomena about knot sizes and explain them by an analytic theory. Our simulations show that short-range intrachain attractions (repulsions) lead to shrinking (swelling) of knot sizes, trends which follow intuition. However, long-range attractions (repulsions) surprisingly lead to swelling (shrinking) of knot sizes. Such counterintuitive trends are because larger knots contain more interacting monomer pairs if the interaction range is larger than a critical value. The critical interaction range varies from a fraction of to multiple persistence lengths, and so the long-range interaction regime can be reached for DNA, peptide chains, or synthetic polymers under depletion attractions induced by colloids (e.g., proteins) or via Coulomb repulsions. Our results suggest that probabilities and sizes of knots can be controlled *independently* through adjusting the range and the strength of intrachain interactions.

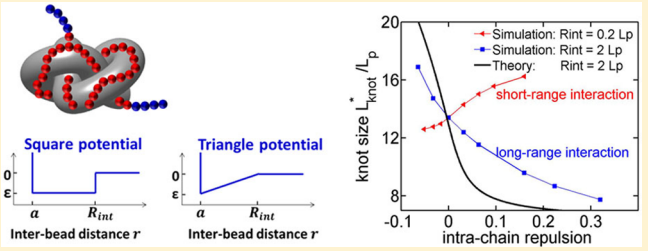

1. INTRODUCTION

We encounter knots in our daily life,[1,2] such as in computer cables or shoelaces. Knots also occur in biopolymers, for example in proteins or DNA.[3−5] The knotting probability of a few kilobase DNA, such as that of a viral genome, is a few percent.[6,7] There are seven natively knotted structures identified from 2936 nonhomology proteins in the protein structure database.[8] Generally, the knotting probability approaches unity as the contour length of a polymer increases. The formation of knots leads to significant consequences, such as jamming polymer translocation through a nanopore[9−11] (relevant to the ejection of DNA from viral capsids[12]), reducing mechanical strengths of polymers,[13] slowing down the coil−stretch transition,[14] and affecting chain dynamics.[15] The knotting in some protein structures may have biological implications.[3,4,16] The investigation of knots under various conditions as well as how to produce knots has been performed in many simulations[17−24] and experiments.[25,26]

There has been little effort devoted to rational controlling of knot properties, such as knotting probability, knot type, knot size, or location of a knot in a chain. In practical applications, one may want to either eliminate or promote knotting in a polymer. For example, knots can decrease resolution when sequencing DNA via linearization in nanofluidic channels.[27,28] Coluzza et al. designed knots in a polymer through the sequence of patches for the application of drug delivery.[23] Very recently, Polles et al. also designed knots by patchy templates.[29]

In this work, we control knots through intrachain interactions. We address a basic question: how do intrachain interactions affect the knotting probability and the knot size in a homopolymer? At first glance, one expects that intrachain repulsions (or attractions) would swell (or shrink) knot sizes. However, our simulations show that the effect of intrachain interaction on the knot size *surprisingly* becomes opposite as the interaction range becomes larger than a critical value. Such unexpected behaviors of knot size induced by intrachain interactions can explain intriguing phenomena reported in two previous simulation studies: (i) Dommersnes et al.[30] found that Coulomb repulsions lead to the shrinking of knot size; (ii) D'Adamo and Micheletti found that depletion attractions by large crowders swell knots.[31] However, these two studies did not reveal the universality of such unexpected behaviors and did not analyze the conditions under which the unexpected behaviors occur. Since the second study[31] focuses on the crowding effects on knots, the authors did not link the swelling of knots by attraction to the shrinking of knots by repulsion.[30] In the current study, we systematically investigate these unexpected behaviors and also explain them by a simple theory. Previously, Dommersnes et al. suggests that Coulomb repulsions tend to swell the overall chain conformation and thus effectively tighten a knot. However, as we will discuss at the end of section 3.4, the repulsion-induced knot tightening in our current study is caused by a mechanism other than the swelling of the entire conformation. We will show that short-range repulsions can swell the overall chain conformation but cannot tighten a knot.

Received: August 1, 2016
Revised: September 16, 2016
Published: September 22, 2016

DOI: 10.1021/acs.macromol.6b01653
Macromolecules 2016, 49, 7581−7587

In the current study, we investigate the effects of intrachain interactions on the knot size and knotting probability, with the focus on the aforementioned unexpected behaviors (knot tightening by repulsions). We also develop a theory to explain the unexpected behaviors.

2. SIMULATION AND THEORY

2.1. Simulation of Polymer Chains. We perform PERM (Pruned-Enriched Rosenbluth Method) simulations[32,33] to generate random conformations for linear semiflexible chains (not circular chains). We then determine the sizes and probabilities of knots using the method in our previous studies.[34−36] The semiflexible chain is modeled as a string of touching beads[37] (Figure 1a). The number of beads is 2000.

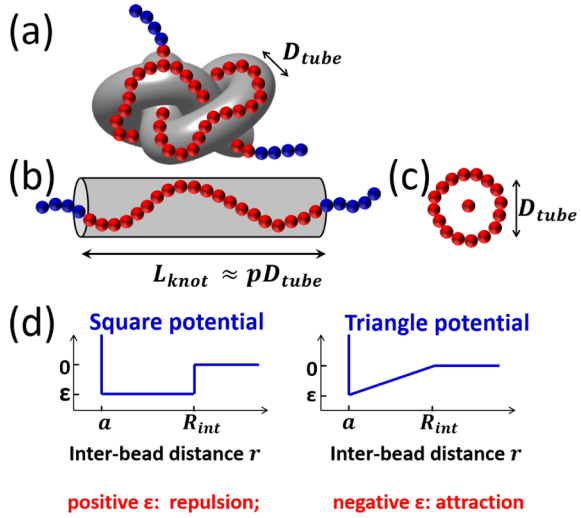

Figure 1. (a) A trefoil knot in a chain. The monomers in the knotted region are marked in red. The gray tube is a virtual tube, in which the red monomers are confined. (b) A chain is confined in a tube. (c) The cross section of the virtual tube. (d) A square/triangle potential is used for intrachain interaction. Positive (negative) values of ϵ correspond to repulsions (attractions).

Bending energies are applied for three adjacent beads to reproduce a persistence length L_p. The pairwise interaction between beads are described as a hard-core repulsion plus either a square potential or a triangle potential. We choose these two simple potentials to speed up simulations as well as for the convenience in theoretical analysis. The square potential is widely used in the modeling of soft matter systems, e.g., hard spheres and polymers. The triangle potential is similar to the depletion potential induced by crowding. The diameter of hard-core a is set as $(1/20)L_p$ unless otherwise specified, so that the parameters are relevant to DNA, which has a persistence length $L_p \approx 50$ nm and a hard-core diameter $a = 2.5$ nm. The depth of the interaction potential at $r = a$ is described by the parameter ϵ.

2.2. Calculation of Knot Sizes. The topology is determined by computing the Alexander polynomial of the chain[38] after closing both ends by a loop based on the minimally interfering closure scheme.[39] The knot core is determined by cutting beads from ends until the topology is changed.

2.3. Theory of Knots in Semiflexible Chains. As proposed by Grosberg and Rabin[40] and validated by our previous simulation,[34] the knot formation in a wormlike chain has two contributions in the free energy:

$$F_{knot}^{wlc} = 17.06(L_{knot}/L_p)^{-1} + 1.86(L_{knot}/L_p)^{1/3} \quad (1)$$

where L_{knot} is the contour length inside the knot core, L_p is the persistence length, and the free energy is in units of thermal energy k_BT hereafter. The first term is the bending energy, and the second term is the confinement free energy due to the subchain in the knot core being confined in a virtual tube (Figure 1a,b). The two prefactors were determined in our prior simulations.[34] The bending energy, scaling as L_{knot}^{-1}, tends to swell a knot, while the confinement free energy, scaling as $L_{knot}^{1/3}$, tends to shrink a knot. The competition of these two energies leads a metastable knot size, corresponding to the free energy minimum.

When taking into account the excluded volume interaction caused by the hard-core diameter of the chain, the free energy of knot formation becomes[34]

$$F_{knot}^{hard} = 17.06(L_{knot}/L_p)^{-1} + 1.86(L_{knot} - 16a)^{-2/3}L_p^{1/3} \quad (2)$$

where the numerical coefficient 16 in the second term was previously determined by simulations.[34]

3. RESULTS AND DISCUSSION

3.1. Simulation Results Using Square Potentials. Figure 2 shows the probability of forming a trefoil knot as a

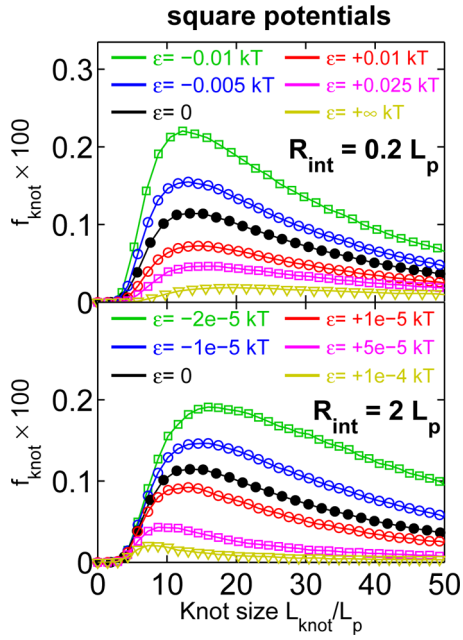

Figure 2. Probability of trefoil knots as a function of knot size in simulations of linear chains using square potentials. The range of intrachain interaction is $R_{int} = 0.2L_p$ (top) and $R_{int} = 2L_p$ (bottom).

function of the rescaled knot size obtained from simulations using square potentials. The contour length is $L = 100L_p$, corresponding to approximately 5 μm DNA. The probability $f_{knot}(x)$ is normalized such that $\int_0^{L/L_p} f_{knot}(x)\,dx = f_{total}$, where $x = L_{knot}/L_p$ and f_{total} is the total probability of forming trefoil knots. For both R_{int}, attractions (repulsions) always increase (decrease) knotting probabilities. However, the metastable knot size L_{knot}^* (peak location) exhibits opposite trends for these two

DOI: 10.1021/acs.macromol.6b01653
Macromolecules 2016, 49, 7581−7587

R_{int}. The attractions with $R_{int} = 0.2L_p$ lead to shrinking of knots, while the attractions with $R_{int} = 2L_p$ surprisingly lead to swelling of knots. The reason why small absolute values of ϵ lead to substantial changes in knotting properties is that ϵ is defined for a pair of monomers. If we convert the interaction strength to that for a pair of persistence-length segments, the interaction strength is comparable to k_BT. Similar trends are observed for flexible chains and other knot types (see Supporting Information).

Figure 3 shows the total probability of forming trefoil knots as a function of the strength of interaction. Note that topology

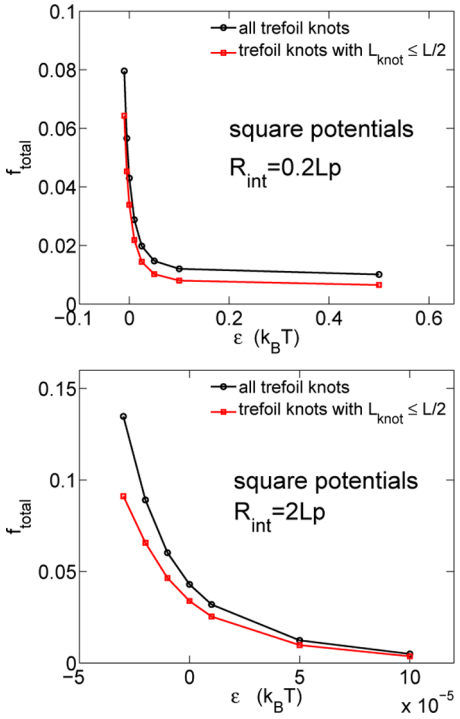

Figure 3. Total probabilities of forming trefoil (3_1) knots in simulations of linear semiflexible chains with $L = 100L_p$ and square potentials: (top) $R_{int} = 0.2L_p$; (bottom) $R_{int} = 2L_p$.

(knot) is strictly defined for circular chains but not for linear chains. A knot in a linear chain can be easily distinguished from unknots if the knot core is localized in a small portion of the chain. Uncertainty in the identification of a knot increases when the knot contains nearly the entire contour length. Such uncertainty disappears as L_{knot} becomes less than $L/2$. As a result, in the calculation of knotting probability, we separately consider all trefoil knots or only the trefoil knots with $L_{knot} \leq L/2$. The effect of intrachain interactions on total knotting probability can be understood by the fact that knot formation leads to more interacting pairs of monomers in the knot core.

3.2. Simulation Results Using Triangle Potentials. Figure 4 shows similar results to Figure 2, except that triangle potentials are used in the simulations. The trends are the same with both type of potentials. In the case of $R_{int} = 0.2L_p$, attractions/repulsions lead to shrinking/swelling of knots. In the case of $R_{int} = 2L_p$, attractions/repulsions lead to opposite trends. The Supporting Information includes the results for $R_{int} = 0.5L_p$, exhibiting the same trend as $R_{int} = 0.2L_p$, and the results $R_{int} = L_p$, where the metastable knot size is insensitive to attractions and repulsions.

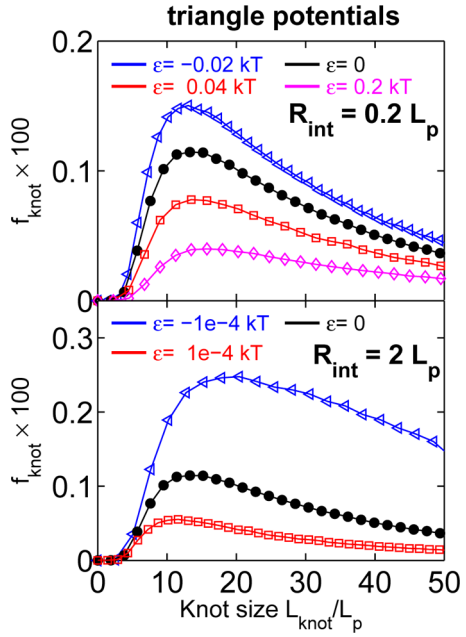

Figure 4. Probability of trefoil knots as a function of knot size in simulations of linear semiflexible chains using triangle potentials. The top and bottom graphs correspond to two interaction ranges: $R_{int} = 0.2L_p$ and $2L_p$, respectively.

3.3. Metastable Knot Sizes. Figure 5 shows the metastable knot size L^*_{knot} as a function of the interaction strength for four

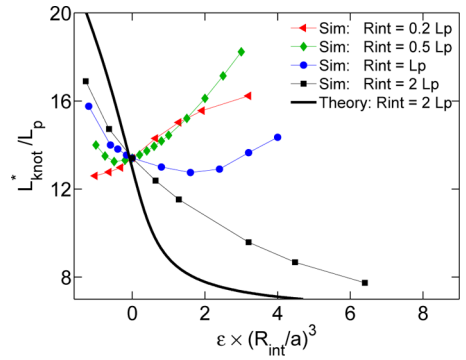

Figure 5. Metastable knot size as a function of the interaction strength from simulations with parameter sets {a linear chain, $N_m = 2000$, a square potential} (symbols) and theory given by eq 10 (thick line).

values of R_{int} (more values of R_{int} can be found in the Supporting Information). The interaction strength is rescaled as $\epsilon_{int} \equiv \epsilon \times (R_{int}/L_p)^3$ primarily for the convenience of comparing different R_{int} in the same plot. Such rescaling would remove the effect of changing R_{int} if the monomers are uniformly distributed in the space. In the case of $R_{int} = 0.2L_p$, L^*_{knot} always increases with ϵ_{int} for $-0.0512 \leq \epsilon_{int} \leq 0.16$. In the case of $R_{int} = 2L_p$, L^*_{knot} always decreases with ϵ_{int} for $-0.064 \leq \epsilon_{int} \leq 0.32$. In cases of $R_{int} = 0.5L_p$ and $R_{int} = L_p$, the curves of L^*_{knot} versus ϵ_{int} have a U-shape, and the critical ϵ_{int} corresponding to the minimal L_{knot} shifts toward larger values for larger R_{int}. We expect that the curves for $R_{int} = 0.2L_p$ and $R_{int} = 2L_p$ also have a U-shape if we plot over a wider range of ϵ. As we decrease ϵ for $R_{int} = 0.2L_p$, polymers will undergo a coil−globule transition, and the knots are no longer localized in globular states,[41−44] i.e., L^*_{knot} approaching a very large value. The attractions plotted in

DOI: 10.1021/acs.macromol.6b01653
Macromolecules 2016, 49, 7581−7587

Figure 5 are not strong enough to induce coil−globule transitions. As we increase ϵ toward $+\infty$ for $R_{int} = 2L_p$, the chain approaches the situation with a hard-core diameter of $2L_p$. In this case, the chain behaves as a flexible chain with monomer size $2L_p$ and has a metastable knot size $L^*_{knot} \approx 280L_p$.[22,35]

Having shown that short-range and long-rang intrachain interactions lead to opposite trends of L^*_{knot}, we determine the critical interaction range R^*_{int} to separate these two regimes, as shown in Figure 6. The value of R^*_{int} can be considered as the

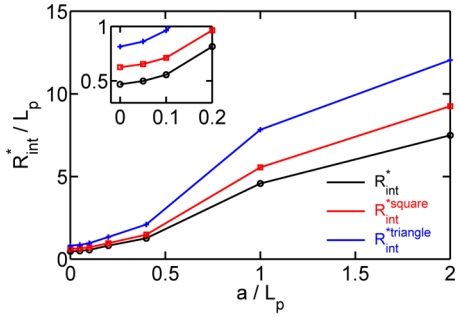

Figure 6. Rescaled critical interaction range as a function of the rescaled hard-core diameter. The values of $R^{*square}_{int}$ and $R^{*triangle}_{int}$ are defined by eqs 6 and 7, respectively.

interaction range which satisfies $\partial L^*_{knot}/\partial\epsilon = 0$ at $\epsilon = 0$. The precise determination of R^*_{int} can be more conveniently done based on the pair correlation of monomers in a chain with $\epsilon = 0$ (see the next subsection). Figure 6 shows that the value of L^*_{knot} increases with the hard-core diameter when we normalize both R^*_{int} and a by L_p. Note that $a/L_p = 2$ in Figure 6 refers to the simulation of flexible chains, while the monomer size is considered as the Kuhn length $2L_p$. Table 1 shows the critical interaction ranges for other knot types. There is no clear trend of R^*_{int} as the knot becomes more complex.

Table 1. Critical Interaction Ranges and the Metastable Knot Sizes for $\epsilon = 0$

knot type	$R^{*square}_{int}/L_p$	$R^{*triangle}_{int}/L_p$	$L^{*\epsilon=0}_{knot}/L_p$
3_1	0.63	0.82	13
4_1	0.37	0.53	24
5_1	0.74	0.95	32
5_2	0.66	0.85	32

[a]The hard-core diameter is $a = (1/20)L_p$.

In addition to the metastable knot size, the mean knot size $\langle L_{knot}\rangle$ is also plotted as a function of ϵ for various R_{int} (see Supporting Information). The trend of $\langle L_{knot}\rangle$ is similar. Note that $\langle L_{knot}\rangle$ often depends on L, while L^*_{knot} does not.[34] The difference between $\langle L_{knot}\rangle$ and L^*_{knot} becomes negligibly small as the knot becomes very tight.

3.4. Theoretical Explanation of Metastable Knot Sizes.

We try to understand the effect of intrachain interactions on knots using a theoretical framework described in section 2.3. In the case of a square potential for the intrachain interaction, we modify the free energy of knot formation to

$$F^{int}_{knot} = 17.06(L_{knot}/L_p)^{-1} + 1.86L_{knot}(L_{knot} - 16a)^{-2/3} \times L_p^{-1/3} + \epsilon N_{int} \quad (3)$$

where N_{int} is the number of monomer pairs within the interaction range $a < r < R_{int}$ at $\epsilon = 0$. Because we consider the ensemble of unknotted states as a reference state, N_{int} refers to the change of contact number induced by knot formation. The first two terms are copied from F^{hard}_{knot} in eq 2 for the free energy of knot formation in a semiflexible chain with purely hard-core repulsion. Since the hard-core repulsion within the range $r < a$ has already been considered in the first two terms, the third term just takes account of the contribution of the interaction in the range $r > a$. The values of ϵ can be positive or negative; i.e., the interaction in the range $r > a$ can be repulsive or attractive. Note that eq 3 assumes that intrachain interactions minus hard-core repulsion are weak perturbations to the energy landscape and hence should be applicable only for $\epsilon N_{int} < 1\ k_BT$. In the case of strong interactions, the above equation should not be applicable. For example, strong attractions lead to the coil−globule transition, and the above equation cannot capture the change of knot size during this transition.

The sign of $\partial N_{int}/\partial L_{knot}$ determines whether intrachain interactions tend to swell or shrink a knot. In the case of a positive value of $\partial N_{int}/\partial L_{knot}$, where larger knots have more interacting pairs of monomers, weak attractions tend to swell knots.

The change in the number of contact pairs N_{int} can be calculated as

$$N^{square}_{int} = \int_a^{R_{int}} [c_{knot}(r) - c_{unknot}(r)]\, dr \quad (4)$$

where $c_{knot}(r)$ and $c_{unknot}(r)$ are the pair correlation functions for knots and unknots. The functions are defined as the number of monomer pairs at the distance r, and so $4\pi r^2$ are absorbed in these functions. If a triangle rather square potential is applied, the effective contact pair is

$$N^{triangle}_{int} = \int_a^{R_{int}} [c_{knot}(r) - c_{unknot}(r)]\frac{R_{int} - r}{R_{int} - a}\, dr \quad (5)$$

Figure 7 shows $\Delta c(r) \equiv c_{knot}(r) - c_{unknot}(r)$ obtained from a simulation with $\epsilon = 0$. The overall shapes of $\Delta c(r)$ are

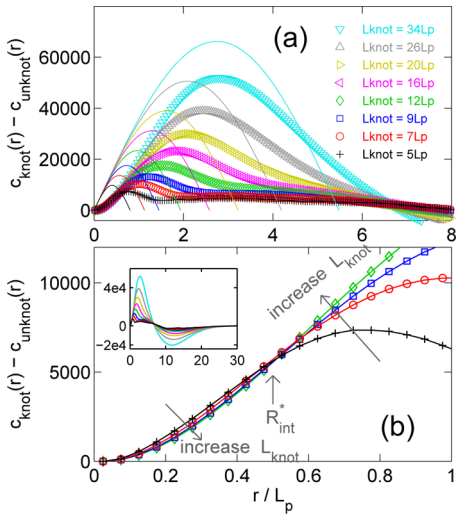

Figure 7. Change of pair correlation induced by the formation of 3_1 knots with different knot sizes. (a) Symbols are obtained from a simulation with $\epsilon = 0$. Solid lines in are theoretical predictions by eq 8. (b) The same simulation data from (a) but plotted in different ranges. For clear viewing, only four curves are included in main plot in (b).

DOI: 10.1021/acs.macromol.6b01653
Macromolecules 2016, 49, 7581−7587

presented in the inset of Figure 7b. The curves for different L_{knot} share a similar shape but with different amplitudes. Such shapes are due to the fact that the formation of knots increases short-distance pairs and decrease long-distance pairs, and the total number of pairs is not changed by knots. Note that the interaction ranges are within in the range $r \leq 2L_p$ where $\Delta c(r)$ is always positive.

We now look into the dependence of $\Delta c(r)$ on L_{knot}, which can be used to infer the dependence of N_{int} on L_{knot}, and then the effect of intrachain interactions on knots. The data in Figure 7a suggest that the number of contact pairs in eq 4 increases with L_{knot} for a sufficiently long-range interaction. It means that for long-range interactions $\partial N_{int}/\partial L_{knot}$ is positive, and attractions/repulsions will lead to swelling/shrinking of knots as observed in Figure 5.

Figure 7b reveals an opposite trend of $\Delta c(r)$ at small r when varying L_{knot}. Increasing L_{knot} will reduce $\Delta c(r)$ at small r. Accordingly, for short-range interactions, $\partial N_{int}/\partial L_{knot}$ is negative, and attractions/repulsions will lead to shrinking/swelling of knots as observed in Figure 5. The critical R^*_{int} separating short-range and long-range interactions is defined by the following equations:

$$\left.\frac{\partial N_{int}^{square}(r)}{\partial L_{knot}}\right|_{L_{knot}=L_{knot}^{*\epsilon=0},r=R_{int}^{*square}} = 0 \tag{6}$$

$$\left.\frac{\partial N_{int}^{triangle}(r)}{\partial L_{knot}}\right|_{L_{knot}=L_{knot}^{*\epsilon=0},r=R_{int}^{*triange}} = 0 \tag{7}$$

Here, $L_{knot}^{*\epsilon=0}$ is the metastable knot size at $\epsilon = 0$, and we have $L_{knot}^{*\epsilon=0} \approx 13L_p$ for trefoil knots with $a/L_p = 0.05$.

The above results and analysis reveal that pair correlations in knots $c_{knot}(r)$ are key factors to understand the effects of intrachain interactions on knots. To derive $c_{knot}(r)$ from theory, we propose a simple model using the idea of a virtual tube (Figure 1a). We assume each monomer in the knotted core is confined by a virtual tube, and tube walls are made of monomers. Then, the pair correlation function in knots is similar to the distribution of monomers in the cross section of a tube (Figure 1c). When the tube diameter D_{tube} is comparable to L_p, the distribution of monomer density can be approximated by a sine function $\sin(\pi x/D_{tube})$, where x is the minimal distance to tube walls (see Supporting Information).[45,46] As a result, we approximate the pair correlation in the knot core $c_{knot}^{core}(r)$ by a sine function:

$$c_{knot}^{core}(r) = A \sin(kr) \tag{8}$$

where

$$A = p\pi L_{knot}/(8a^2) \quad \text{and} \quad k = p\pi/(2L_{knot}) \tag{9}$$

The values of A and k are determined based on two conditions: (i) the density peak should be located at $r_{peak} = D_{tube} = L_{knot}/p$, where $p \approx 12.4$ is an intrinsic parameter[47] for trefoil knots to describe the ratio of the contour length L_{knot} to the tube diameter D_{tube} in the virtual-tube model; (ii) the total number of pairs in knots is $\int_0^{2r_{peak}} \Delta c(r)\, dr = (1/2)(L_{knot}/a)^2$. The solid lines in Figure 7 demonstrate that eq 8 captures the general shapes of $\Delta c(r)$ in Figure 7 and the dependence of $\Delta c(r)$ on L_{knot}. The amplitudes of $c_{knot}^{core}(r)$ are close to $\Delta c(r)$, which implies $\Delta c(r)$ is dominated by $c_{knot}(r)$. Hence, we approximate $\Delta c(r) \approx c_{knot}^{core}(r)$.

Substituting eqs 8 and 4 into eq 3, we obtain

$$F_{knot} = 17.06\frac{L_p}{L_{knot}} + 1.86\frac{L_{knot}}{(L_{knot} - 16a)^{2/3}L_p^{1/3}} + \epsilon\frac{L_{knot}^2}{4L_p^2}\left[1 - \cos\left(\frac{p\pi}{2L_{knot}}R_{int}\right)\right] \tag{10}$$

Minimization of F_{knot} with respect to L_{knot} yields the metastable knot sizes. On the basis of this equation, we calculate L_{knot} for $R_{int} = 2L_p$ with no fitting parameter as shown by the solid line in Figure 5. The theoretical prediction captures the effect of long-range intrachain interactions on the metastable knot size.

However, eq 10 cannot explain the effect of short-range interactions on L^*_{knot} because eq 8 fails to produce negative values of $\partial c_{knot}(r)/\partial L_{knot}$ at small r. Such a limitation of the theory is not surprising because the derivation of $c_{knot}(r)$ using the virtual tube makes many simplifications. Here, we enumerate the approximations in our theory to calculate L^*_{knot}. First, the free energy expression for a chain with purely hard-core repulsions $F_{knot} = 17.06(L_{knot}/L_p)^{-1} + 1.86L_{knot}(L_{knot} - 16a)^{-2/3}L_p^{-1/3}$ is relatively precise to calculate the metastable knot size but is not precise to predict the spring constant around L^*_{knot}. This means that even if we can precisely calculate ϵN_{int}, the calculated L^*_{knot} for a given ϵ may be not precise. Second, the virtual tube model is an approximation, and it is based on an ideal knot conformation (maximally inflated knot). Third, we use a sine function for the pair correlation, but in reality the distribution function of the monomer density rather than the pair correlation function is close to an sine function (see Supporting Information). If we assume every bead in the knot core is confined by a tube wall consisting of uniformly distributed beads, then the pair correlation becomes similar to the distribution of monomers density in a tube. Fourth, for the pair function defined in eq 4, a factor of $4\pi r^2$ should be absorbed inside. We find that the factor $\sim r^2$ is not needed in $c_{knot}^{core}(r)$ to fit the simulation results in Figure 7. If we use a function form $c_{knot}^{core} \sim \sin(kr)r^2$, then we fail to capture the collapse of different curves for different L_{knot} at small r. Fifth, the distribution of monomers of wormlike chains in the circular cross sections of tubes depends on the ratio R_{tube}/L_p (see Supporting Information). As the tube diameter decreases, the segments becomes more likely to locate close to walls. When the tube diameter is a few times of L_p, the distribution is close to an sine function. The dependence of this distribution on R_{tube}/L_p might lead to the trend of $c(r)$ at r when varying L_{knot}.

It is worthy mentioning that Dommersnes et al.[30] explained the knot shrinking induced by long-range repulsions through a mechanism in which repulsions swell the chain and then tighten a knot. Such mechanism explained their specific observations but appears not to be the reason for our observations due to three facts. First, short-range repulsions can swell the overall chain conformation to the same extent as the one by long-range repulsions, but they can lead to knot swelling (Figure 8). Second, very strong long-range repulsion leads to knot swelling rather than knot shrinking as shown by the blue line in Figure 5. Third, our simulations show that L^*_{knot} is insensitive to the contour length L of the entire chain, i.e., L^*_{knot} is a *local* property, while the explanation by Dommersnes et al.[30] suggests L^*_{knot} depends on L.

3.5. Relevance of Our Results in Biopolymers. Lastly, we discuss the relevance of our results to experimental and biological systems. For double-stranded DNA with a hard-core diameter $a \approx 2.5$ nm and persistence length $L_p \approx 50$ nm, the

DOI: 10.1021/acs.macromol.6b01653
Macromolecules 2016, 49, 7581−7587

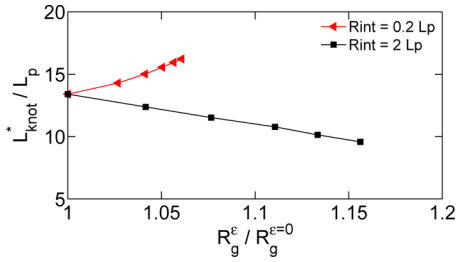

Figure 8. Metastable knot size versus the radius of gyration when varying ϵ. The red and black symbols correspond to chains with short-range and long-range repulsive interactions, respectively.

critical interaction range for a triangle potential is around 43 nm. Considering that the depletion attraction induced by crowders is close to a triangle potential, the long-range interaction regime for DNA can be achieved by crowders larger than 43 nm, which is close to the dextran (crowder) size 34 nm (twice of radius of gyration) used in DNA experiments.[48,49] For flexible chains, such as synthetic polymers, peptide chains, or single-stranded DNA, the monomer size is on the order of a nanometer, and thus the critical interaction range $R_{int}^{*triangle} \approx 6.0a$ is only a few nanometers.

Recently, D'Adamo and Micheletti[31] observed that knots in flexible chains become more abundant in the presence of crowders. The crowders with size $15a$ and $10a$ lead to a significant increase of the knot size, while the knot size is insensitive to the crowders with size $7.3a$. All of these observations are consistent with $R_{int}^{*triangle} \approx 6.0a$ obtained in the current study.

4. CONCLUSIONS

In conclusion, we find that short-range and long-range intrachain interactions lead to opposite behaviors in determining the knot sizes in polymers. This phenomenon arises because larger knots contain more long-distance segment pairs and less short-distance segment pairs than smaller knots. There are two length scales in the polymer model—the monomer size a and the persistence length L_p—and the interaction range in the current study is defined with respect to a and L_p. The critical interaction range depends on the persistence length and the hard-core diameter and can range from a few nanometer to tens of nanometers. Hence, the long-range interaction regime can be achieved in experiments of DNA, peptide chains, and other polymers. The theoretical derivation of the critical interaction range requires a rigorous calculation of the short-distance pair correlation function in knots, which may be resolved in a future study.

An interesting observation in our study is that attractions (repulsions) always increase (decrease) knotting probabilities no matter if the interactions are short-range or long-range. As a result, probabilities and sizes of knots can be controlled independently by adjusting the range of the intrachain interaction.

For the sake of efficient simulation and straightforward theoretical analysis, we employ two simple potentials: rectangle and triangle potentials. In future studies, realistic potentials can be used, in particular, the Yukawa potential for screened electrostatic interactions.

■ ASSOCIATED CONTENT

Supporting Information

The Supporting Information is available free of charge on the ACS Publications website at DOI: 10.1021/acs.macromol.6b01653.

More simulation results of knot sizes for other interaction parameters and distribution of wormlike chains in tubes (PDF)

■ AUTHOR INFORMATION

Corresponding Author

*E-mail: pdoyle@mit.edu (P.S.D.).

Notes

The authors declare no competing financial interest.

■ ACKNOWLEDGMENTS

This research was supported by the National Research Foundation Singapore through the Singapore MIT Alliance for Research and Technology's research program in BioSystems and Micromechanics and the National Science Foundation (Grant CBET-1602406).

■ REFERENCES

(1) Belmonte, A.; Shelley, M. J.; Eldakar, S. T.; Wiggins, C. H. Dynamic Patterns and Self-Knotting of a Driven Hanging Chain. *Phys. Rev. Lett.* **2001**, *87*, 114301.
(2) Raymer, D. M.; Smith, D. E. Spontaneous knotting of an agitated string. *Proc. Natl. Acad. Sci. U. S. A.* **2007**, *104*, 16432−16437.
(3) Taylor, W. R. A deeply knotted protein structure and how it might fold. *Nature* **2000**, *406*, 916−919.
(4) Virnau, P.; Mirny, L. A.; Kardar, M. Intricate knots in proteins: Function and evolution. *PLoS Comput. Biol.* **2006**, *2*, e122.
(5) Mallam, A. L.; Jackson, S. E. Knot formation in newly translated proteins is spontaneous and accelerated by chaperonins. *Nat. Chem. Biol.* **2012**, *8*, 147−153.
(6) Shaw, S. Y.; Wang, J. C. Knotting of a DNA chain during ring closure. *Science* **1993**, *260*, 533−536.
(7) Rybenkov, V. V.; Cozzarelli, N. R.; Vologodskii, A. V. Probability of DNA knotting and the effective diameter of the DNA double helix. *Proc. Natl. Acad. Sci. U. S. A.* **1993**, *90*, 5307−5311.
(8) Dai, L.; Zhou, Y. Characterizing the existing and potential structural space of proteins by large-scale multiple loop permutations. *J. Mol. Biol.* **2011**, *408*, 585−595.
(9) Huang, L.; Makarov, D. E. Translocation of a knotted polypeptide through a pore. *J. Chem. Phys.* **2008**, *129*, 121107.
(10) Szymczak, P. Translocation of knotted proteins through a pore. *Eur. Phys. J.: Spec. Top.* **2014**, *223*, 1805−1812.
(11) Rosa, A.; Di Ventra, M.; Micheletti, C. Topological jamming of spontaneously knotted polyelectrolyte chains driven through a nanopore. *Phys. Rev. Lett.* **2012**, *109*, 118301.
(12) Matthews, R.; Louis, A.; Yeomans, J. Knot-controlled ejection of a polymer from a virus capsid. *Phys. Rev. Lett.* **2009**, *102*, 088101.
(13) Saitta, A. M.; Soper, P. D.; Wasserman, E.; Klein, M. L. Influence of a knot on the strength of a polymer strand. *Nature* **1999**, *399*, 46−48.
(14) Renner, C. B.; Doyle, P. S. Stretching self-entangled DNA molecules in elongational fields. *Soft Matter* **2015**, *11*, 3105−3114.
(15) Tang, J.; Du, N.; Doyle, P. S. Compression and self-entanglement of single DNA molecules under uniform electric field. *Proc. Natl. Acad. Sci. U. S. A.* **2011**, *108*, 16153−16158.
(16) Meluzzi, D.; Smith, D. E.; Arya, G. Biophysics of knotting. *Annu. Rev. Biophys.* **2010**, *39*, 349−366.
(17) Vologodskii, A. Brownian dynamics simulation of knot diffusion along a stretched DNA molecule. *Biophys. J.* **2006**, *90*, 1594−1597.

DOI: 10.1021/acs.macromol.6b01653
Macromolecules 2016, 49, 7581−7587

(18) Orlandini, E.; Whittington, S. G. Statistical topology of closed curves: Some applications in polymer physics. *Rev. Mod. Phys.* **2007**, *79*, 611.
(19) Dai, L.; van der Maarel, J. R.; Doyle, P. S. Effect of nanoslit confinement on the knotting probability of circular DNA. *ACS Macro Lett.* **2012**, *1*, 732−736.
(20) Matthews, R.; Louis, A. A.; Likos, C. N. Effect of Bending Rigidity on the Knotting of a Polymer under Tension. *ACS Macro Lett.* **2012**, *1*, 1352−1356.
(21) Micheletti, C.; Orlandini, E. Knotting and metric scaling properties of DNA confined in nano-channels: a Monte Carlo study. *Soft Matter* **2012**, *8*, 10959−10968.
(22) Tubiana, L.; Rosa, A.; Fragiacomo, F.; Micheletti, C. Spontaneous knotting and unknotting of flexible linear polymers: equilibrium and kinetic aspects. *Macromolecules* **2013**, *46*, 3669−3678.
(23) Coluzza, I.; van Oostrum, P. D.; Capone, B.; Reimhult, E.; Dellago, C. Sequence controlled self-knotting colloidal patchy polymers. *Phys. Rev. Lett.* **2013**, *110*, 075501.
(24) Poier, P.; Likos, C. N.; Matthews, R. Influence of Rigidity and Knot Complexity on the Knotting of Confined Polymers. *Macromolecules* **2014**, *47*, 3394−3400.
(25) Arai, Y.; Yasuda, R.; Akashi, K.-i.; Harada, Y.; Miyata, H.; Kinosita, K.; Itoh, H. Tying a molecular knot with optical tweezers. *Nature* **1999**, *399*, 446−448.
(26) Metzler, R.; Reisner, W.; Riehn, R.; Austin, R.; Tegenfeldt, J.; Sokolov, I. M. Diffusion mechanisms of localised knots along a polymer. *Europhys. Lett.* **2006**, *76*, 696.
(27) Reinhart, W. F.; Reifenberger, J. G.; Gupta, D.; Muralidhar, A.; Sheats, J.; Cao, H.; Dorfman, K. D. Distribution of distances between DNA barcode labels in nanochannels close to the persistence length. *J. Chem. Phys.* **2015**, *142*, 064902.
(28) Reifenberger, J. G.; Dorfman, K. D.; Cao, H. Topological events in single molecules of E. coli DNA confined in nanochannels. *Analyst* **2015**, *140*, 4887−4894.
(29) Polles, G.; Marenduzzo, D.; Orlandini, E.; Micheletti, C. Self-assembling knots of controlled topology by designing the geometry of patchy templates. *Nat. Commun.* **2015**, *6*, 6423.
(30) Dommersnes, P. G.; Kantor, Y.; Kardar, M. Knots in charged polymers. *Phys. Rev. E: Stat. Phys., Plasmas, Fluids, Relat. Interdiscip. Top.* **2002**, *66*, 031802.
(31) D'Adamo, G.; Micheletti, C. Molecular Crowding Increases Knots Abundance in Linear Polymers. *Macromolecules* **2015**, *48*, 6337−6346.
(32) Grassberger, P. Pruned-enriched Rosenbluth method: Simulations of θ polymers of chain length up to 1 000 000. *Phys. Rev. E: Stat. Phys., Plasmas, Fluids, Relat. Interdiscip. Top.* **1997**, *56*, 3682.
(33) Dai, L.; van der Maarel, J.; Doyle, P. S. Extended de Gennes Regime of DNA Confined in a Nanochannel. *Macromolecules* **2014**, *47*, 2445−2450.
(34) Dai, L.; Renner, C. B.; Doyle, P. S. Metastable Tight Knots in Semiflexible Chains. *Macromolecules* **2014**, *47*, 6135−6140.
(35) Dai, L.; Renner, C. B.; Doyle, P. S. Origin of Metastable Knots in Single Flexible Chains. *Phys. Rev. Lett.* **2015**, *114*, 037801.
(36) Dai, L.; Renner, C. B.; Doyle, P. S. Metastable Knots in Confined Semiflexible Chains. *Macromolecules* **2015**, *48*, 2812−2818.
(37) Dai, L.; Jones, J. J.; van der Maarel, J. R.; Doyle, P. S. A systematic study of DNA conformation in slitlike confinement. *Soft Matter* **2012**, *8*, 2972−2982.
(38) Frank-Kamenetskii, M.; Vologodskii, A. Topological aspects of the physics of polymers: The theory and its biophysical applications. *Soviet Physics Uspekhi* **1981**, *24*, 679.
(39) Tubiana, L.; Orlandini, E.; Micheletti, C. Probing the entanglement and locating knots in ring polymers a comparative study of different arc closure schemes. *Prog. Theor. Phys. Supp* **2011**, *191*, 192.
(40) Grosberg, A. Y.; Rabin, Y. Metastable tight knots in a wormlike polymer. *Phys. Rev. Lett.* **2007**, *99*, 217801.
(41) Orlandini, E.; Stella, A.; et al. Orlandini, E and Stella, AL and others Loose, flat knots in collapsed polymers. *J. Stat. Phys.* **2004**, *115*, 681−700.
(42) Marcone, B.; Orlandini, E.; Stella, A.; Zonta, F. What is the length of a knot in a polymer? *J. Phys. A: Math. Gen.* **2005**, *38*, L15.
(43) Virnau, P.; Kantor, Y.; Kardar, M. Knots in globule and coil phases of a model polyethylene. *J. Am. Chem. Soc.* **2005**, *127*, 15102−15106.
(44) Kardar, M. The elusiveness of polymer knots. *Eur. Phys. J. B* **2008**, *64*, 519−523.
(45) Werner, E.; Westerlund, F.; Tegenfeldt, J. O.; Mehlig, B. Monomer distributions and intrachain collisions of a polymer confined to a channel. *Macromolecules* **2013**, *46*, 6644−6650.
(46) Chen, J. Z. Free Energy and Extension of a Wormlike Chain in Tube Confinement. *Macromolecules* **2013**, *46*, 9837−9844.
(47) Pierański, P.; Przybył, S.; Stasiak, A. Tight open knots. *Eur. Phys. J. E: Soft Matter Biol. Phys.* **2001**, *6*, 123−128.
(48) Zhang, C.; Shao, P. G.; van Kan, J. A.; van der Maarel, J. R. Macromolecular crowding induced elongation and compaction of single DNA molecules confined in a nanochannel. *Proc. Natl. Acad. Sci. U. S. A.* **2009**, *106*, 16651−16656.
(49) Jones, J. J.; van der Maarel, J. R.; Doyle, P. S. Effect of nanochannel geometry on DNA structure in the presence of macromolecular crowding agent. *Nano Lett.* **2011**, *11*, 5047−5053.

DOI: 10.1021/acs.macromol.6b01653
Macromolecules 2016, 49, 7581−7587